JOURNAL OF PROPULSION AND POWER
Vol. 26, No. 5, September–October 2010

High-Performance Rocket Nozzle Concept

Luca Boccaletto*
ESA, 2201 AZ Noordwijk, The Netherlands
and
Jean-Paul Dussauge†
Université de Provence, 13453 Marseille Cedex 13, France

DOI: 10.2514/1.48904

An innovative technical solution that overcomes the limitation induced by flow separation phenomena and allows increasing the vacuum-specific impulse of a main stage rocket engine is presented. After reviewing the open technical literature on flow separation and advance nozzles design, the newly proposed concept is extensively presented. Three-dimensional computational fluid dynamics analyses and experimental results (cold gas subscale models) demonstrate the effectiveness of a simple device, adaptable to any bell-shaped nozzle and which provides a solution to the flow separation issue, while increasing vacuum-specific impulse performances for booster and main stage engines. Moreover, this new concept gives rise to a wider engine-throttling range, even at low altitude, without incurring flow separation and associated side loads. Experimental data show a potential for favorable behavior even during transient phases, allowing significant reduction on transient side-loads activity. Finally, three-dimensional computational fluid dynamics computations have been extended to the hot firing case (chemically reactive hydrogen/oxygen propellants), both in steady-state and transient conditions. The results show the suitability of the proposed concept for application to real rocket engines.

Nomenclature

k	=	mean turbulent kinetic energy, $(m/s)^2$
L	=	length of nozzle supersonic part, m
P_{ij}	=	aerospike stagnation pressure, Pa
P_{cc}	=	combustion chamber stagnation pressure, Pa
X	=	axial coordinate, m
ε	=	mean turbulent kinetic energy dissipation rate, W/kg

I. Introduction

PERFORMANCE optimization is one of the main drivers for space launchers design. To achieve this objective, the dry mass of the vehicle must be as low as possible and all the subsystems and equipments must meet highest efficiency requirements. Between all, propulsion systems are the most critical parts of a launcher and their efficiency is a key parameter to put large payloads into orbit. For upper stage engines, specific impulse is usually the main parameter to be optimized whereas for main stage and booster engines thrust is the key parameter for the initial ascending phase and specific impulse becomes more important as soon as the vehicle reaches higher altitudes and speed. Therefore, for a given propellant couple and for a given thermodynamic engine cycle, main stage engines are designed in order to meet maximum thrust requirements and to optimize specific impulse at high altitude, always operating in safe mode, especially with regard to flow separation issues.

Indeed, flow separation phenomenon, in particular at sea level, is a major constraint for optimization of main engine nozzles. For decades, scientists and engineers have been working on nozzle flow separation trying to better understand the physics of this phenomenon and to reduce associated thermal and mechanical loads. At the same time, alternative nozzle configurations have been proposed in order to avoid flow separation while increasing engine performances. Nevertheless, despite the variety of concepts already proposed in the technical literature, the majority of present launch systems use conventional bell-shaped nozzles; innovative concepts have only been tested on ground or have equipped small experimental rockets. This is mostly due to reliability constraints imposed on heavy launch systems as well as to the technical complexity related to some of these advanced concepts, like aerospike or adaptive devices such as dual bell and deployable nozzles. Therefore, vacuum performances of main stage rocket engines remain limited by design constrains related to operating conditions at sea level. In other terms, existing rocket nozzles are designed to operate in adapted conditions when the external pressure is equal to about one third of the ambient pressure at sea level; that definitely represents a strong limitation in performance optimization with respect to vacuum-specific impulse.

In this paper an innovative technical solution overcoming the limitation induced by flow separation phenomena and allowing improvement of the vacuum-specific impulse for main stage rocket engines is presented.

A brief review of the relevant open literature is discussed in the following section. Then, the proposed device is described; computational and experimental results obtained on a subscale cold gas model are presented. These results confirm the effectiveness of a device simply adaptable to any bell-shaped nozzle, which solves the flow separation issue, while allowing increased vacuum-specific impulse for booster and main stage engines. As a final verification, computational fluid dynamics (CFD) computations have been carried out for a chemically reactive oxygen/hydrogen propellants case. Steady-state and transient behavior have been analyzed and checked. The results show the suitability of such a device for application to a real rocket engine.

II. Background and Basic Descriptions

Flow separation in supersonic nozzles originates at the wall as a consequence of the adverse pressure gradient experienced by the boundary layer, when the supersonic expansion is large enough to reduce wall static pressure at some value, lower than the ambient one. This phenomenon occurs every time that a rocket nozzle is operated in transient conditions (start-up or shut-down) and can originate

Received 12 January 2010; revision received 27 May 2010; accepted for publication 9 June 2010.

*Propulsion Engineer, European Space Research and Technology Center, Keperlaan 1-2201 AZ; Luca.Boccaletto@esa.int.

†Director of Research, Centre National de la Recherche Scientifique, IUSTI, Supersonic Group 5, Rue Enrico Fermi; jean-paul.dussauge@polytech.univ-mrs.fr.

during steady-state conditions if the nozzle expansion ratio is large enough.

A. Literature Survey

A considerable amount of work has been done since the middle of the last century [1] in order to better understand flow separation in supersonic nozzles and intense activities are still progressing in several countries. The flow separation control device and the Aérothermodynamique des Tuyères et Arrière Corps research groups are active in Europe (see [2,3]) and research activities are also ongoing in the United States, as reported in [4–7], as well as in Japan (see [8,9]).

Several works carried out in the past were mainly focused on the detailed characterization of the flow separation phenomenology, while other authors tried to refine already existing engineering criteria for nozzle design, aiming at maximizing the nozzles expansion ratio without incurring in flow separation when operated at sea level. Recently, a comprehensive compilation of all the proposed criteria (mostly empirical or semi-empirical) has been gathered by Stark (see [10]). From the comprehensive study of Stark, it appears quite evident that experimental data are scattered and the flow separation occurrence depends on several parameters: the nozzle profile, wall actual conditions (roughness, waviness, geometrical defects), engine operating conditions and gas chemical composition. Nevertheless, that study clearly shows that wall static pressure values at which the flow separates usually range from 0.25 to 0.4 times the ambient pressure level.

Other studies available in the open literature emphasize the major role played by the external ambient pressure on flow separation occurrence. Accordingly, the ratio between wall static pressure (at nozzle outlet) and atmospheric pressure is commonly used as an efficient parameter for correlations to predict flow separation appearance. Nevertheless, in most of the available scientific works, the basic physical mechanism initiating the flow separation is rarely investigated [11–13], resulting in a very limited number of ideas to suppress this undesirable phenomenon. Only design limitations for bell-shaped nozzles have clearly been highlighted by the previous studies.

Concerning alternative nozzle concepts, some configurations have been proposed in the past, aiming at removing the flow separation issue and its consequences: few ideas are based on slight modifications to be introduced in classical bell-shaped nozzles [14,15]; scarce success was obtained. Other concepts have been proposed and tested, aiming at the evaluation of the efficiency of compensating devices like dual bell nozzles [16] or deployable nozzles [17]. Alternative geometries like aerospike nozzles [18] or expansion deflection nozzles [19] have also been largely investigated.

Despite the increasing interest in recent years on dual bell nozzles [16,20,21], these devices present some major drawbacks, namely the uncertainty on the actual transition altitude [22] as well as the severe side-loads which can develop during the operation in first mode (detached flow at inflection area) and during transition.

Deployable nozzles for main stage engines would require heavy and unreliable deployment mechanisms, while aerospike nozzle suffers of quite poor performances at high altitude, in addition to the technological challenges that have to be solved for this kind of concept (cooling, flow pattern control, materials' selection).

Finally, expansion deflection nozzles are extremely constraining for the global engine mechanical layout, and they are not realistically applicable to engines of large size.

For a more detailed discussion on these topics, [23] provides a comprehensive overview of nozzles technology and related flow separation issues.

B. New Concept

Based on the previous considerations, this study originated with the purpose to investigate the possibility to overcome the flow separation issue and, preferably, to definitely suppress this intrinsic limitation for a classical over expanded bell nozzle, at least during steady-state operation. The starting point consisted in keeping the bell-shaped nozzle profile as a working baseline. Indeed, its performances and its global behavior are well known and flight proven. Therefore, this study investigates the possibility to remove the root causes which initiate the flow separation and the behavior of the modified nozzle operating at higher expansion ratios.

After some trial-and-error iterations, it became evident that a very small device, added on the external surface of the nozzle outlet region, could provide surprising and very attractive results. Indeed, the flow separation can be considered as the ultimate effect of an adverse pressure gradient acting on the supersonic boundary layer: the boundary layer is progressively decelerated and the velocity profile is eventually inverted. Therefore, the boundary layer thickness increases and the flow locally separates, generating a shock wave which originates near the wall and penetrates into the supersonic jet. The pressure jump through the shock wave enhances the adverse pressure gradient, enforcing the local separation and producing a massive flow separation. Once the free shock separation (FSS) is settled, a strong recirculation stream, fed by ambient air, occupies the separated area and sustains the separated flow configuration. It is important to notice that the sustenance of the flow separation is only possible if the recirculating bubble is permanently fed.

Therefore, the problem can be solved just stopping (or preventing from the beginning) the presence of a recirculating flow: if the external air cannot flow into the separated annulus the recirculation bubble is not more sustained and the separated supersonic plume quickly drains away the low momentum pocket. Thus, the local pressure decreases again and the adverse pressure gradient is removed.

The question is then: how to prevent external air flowing inside the nozzle, in particular in the separated annulus?

The solution has been found simply by conjugating the basic shaped nozzle geometry with a very small aerospike device positioned around the nozzle lip. The annular aerospike flow (also called secondary flow in this paper) acts like a high momentum fluidic barrier, which cannot be penetrated by ambient air, even under the action of the worst pressure difference (1 bar maximum, at sea level conditions). This fluidic barrier can only be deflected toward the separated main jet, creating a closed annular bubble which is rapidly emptied by the draining action of the plume.

This simple consideration does not apply to typical dump cooled nozzles, because of the limited fluidic efficiency of the exhausted coolant flow. Indeed, in this case the secondary flow is characterized by high static pressure and relatively low momentum and it is evacuated trough a series of nozzlets which generates a discontinuous fluidic barrier.

From a mechanical point of view, the small annular aerospike can easily be implemented in all the existing bell nozzles, without major impacts on its robustness (it can even be used as an integral stiffener) and on its thermal and operational features.

As discussed in following sections, the effectiveness of such a device has been proven to be unexpectedly high even for small mass flow rates of the secondary jet: when the aerospike is operated, full-flowing conditions of the main jet can be achieved at very low pressure ratios.

Figure 1 shows the concept outlines.

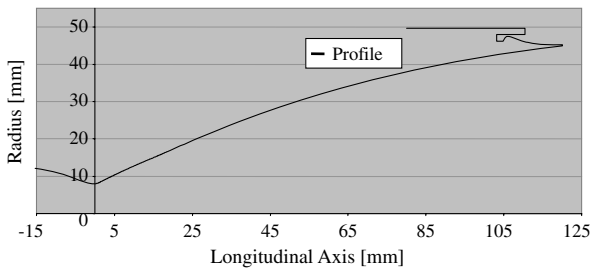

Fig. 1 Actual profile used for computational and experimental investigations.

III. CFD Verification

The nozzle concept herein proposed is the result of an exhaustive evaluation of open technical literature and is based on simple qualitative considerations. Thus, in order to confirm the engineering judgment and quantify the concept effectiveness, a series of two-dimensional CFD computations have been done.

The model has been developed under the CPS-C environment [24], which is a finite-volume software package designed to analyze complex physical processes in fluids. CPS-C is designed to solve aerodynamic flow models based on either compressible or incompressible flows. High-Mach flows with shock waves can be modeled with great accuracy in time and space using a decomposition scheme for transport equations. The underlying mathematical model is based on the mass averaged Navier–Stokes equation written for compressible multispecies reacting flows. Viscous effects are taken into account and various turbulent models are included in the software package. This code has been used on a number of elementary test cases, as well as full-scale applications [25].

It must be underlined that two-dimensional computations under CPS-C environment are considered a special case of a more general three-dimensional simulation (only one element is implemented in the third direction).

Subsequently, additional computations have also been performed on a fully three-dimensional mesh, in order to confirm assessments based on two-dimensional computations.

A. Preliminary Two-Dimensional Model

The preliminary two-dimensional model uses about 7000 elements, mostly hexahedral, and principally distributed in the supersonic part of the nozzle. The turbulence model is a high Reynolds number model (k, ε like), with compressibility correction. As demonstrated by Durbin [26] and Poroseva and Iaccarino [27], such a turbulence model gives very good results even for separated flows. A wall function approach has been chosen for the treatment of the near-wall flow field. Reference [28] provides a detailed discussion about effectiveness of wall functions for this kind of computations.

The nozzle inner geometry is a thrust optimized contour (TOC) profile, similar to that already used in previous numerical and experimental studies [29].

To confirm the validity of the proposed concept and to avoid any optimistic and premature conclusion, a worst case approach is adopted in this study: a low efficiency aerospike contour is selected (excessive length, low expansion ratio of shrouded part) [30]; thickness of the main nozzle lip is kept high (0.4 mm at 1:20 scale with respect to actual rocket engines' size), allowing appearance of a disturbing base flow region at the confluence of the two supersonic jets. Reduced mass flow rate for the annular aerospike (less than 5% of the main nozzle mass flow rate at full-flowing conditions) and severe operating conditions for the main nozzle [nozzle pressure ratio (NPR) set at around 50% of the full-flowing conditions] have been selected for the computed test case. Even under these constraining conditions, very satisfactory results have been obtained. Indeed, when the main nozzle is normally operated, full-flowing condition are reached at NPR of about 75; in case the annular aerospike is also operated, full-flowing conditions can be maintained (in the main nozzle) for NPR values down to 35.

To illustrate the concept effectiveness, Figs. 2 and 3 show the computed pressure field (relative values) for the main nozzle operating at following conditions: the working media is air at NPR 40, the stagnation temperature is set at 1500 K. The annular aerospike is represented only for the case presented in Fig. 3. Stagnation pressure of the annular aerospike is set at 5 bar, while stagnation temperature is fixed at 600 K. Ambient conditions are set at 1 bar, 300 K. Figure 3 clearly shows that the shock wave is displaced forward by the action of the annular jet and the flow separation disappears. Results presented in Figs. 2 and 3 are intended for qualitative evaluation only; a more detailed discussion on CFD results is given in the following section.

Fig. 2 Flow separation in classical bell-shaped nozzles (pressure field, relative scale).

Fig. 3 Full-flowing modified nozzle (pressure field, relative scale).

B. Three-Dimensional Model

Additional test cases have been computed with a three-dimensional CFD model. The TOC nozzle profile used for these computations is slightly different from that used for two-dimensional studies, allowing better representativeness of the Mach field relevant to real engines (in hot gas conditions). The same profile has been used for the experimental activities discussed in Sec. IV. The same aerospike geometry used for two-dimensional studies is implemented in the three-dimensional model.

A tightly unstructured mesh with an angular resolution of 3 deg is used for the computations. The final model features about 71,000 elements, mostly hexahedral and principally distributed inside the main nozzle and in the area of the external annular aerospike. The three-dimensional model represents a 18-deg angular sector of the proposed concept. Moreover, the nozzle external geometry is slightly modified with respect to two-dimensional mesh, in order to better represent the actual geometrical layout of the experimental device, which has been used for cold test experiments (see Sec. IV).

A Roe–Toumi second-order strengthened scheme (default CPS − C scheme) has been chosen for three-dimensional computations [24]. The turbulence model is the same used for the two-dimensional computations, as well as wall function model.

Figure 4 shows the three-dimensional nozzle mesh.

The flow field characteristics have been investigated in detail, with particular attention to the three-dimensional features of the main jet, as well as of the annular flow and their interaction. Results obtained from three-dimensional model confirmed the effectiveness of the proposed concept.

Figure 5 shows the pressure field around the main nozzle lip, for operating conditions similar to those described in Sec. III.A. The flow inside the main jet remains attached up to the nozzle end, even at low NPR (35). It should be noticed that the flow field generated by the annular aerospike is coherent with classical results available in open literature (see [30]). In addition, the pressure field surrounding the annular aerospike flow is not disturbed by the presence of the tick flange introduced in the test article design, due to manufacturing constraints.

In the absence of the secondary flow, the separation line is located at about $X/L = 0.63$.

The minimum wall pressure calculated near the nozzle lip is about 16,000 Pa, i.e., much less than the lowest pressure level ever measured in a classical bell-shaped nozzle operating at sea level, since the flow already separates at higher pressure levels.

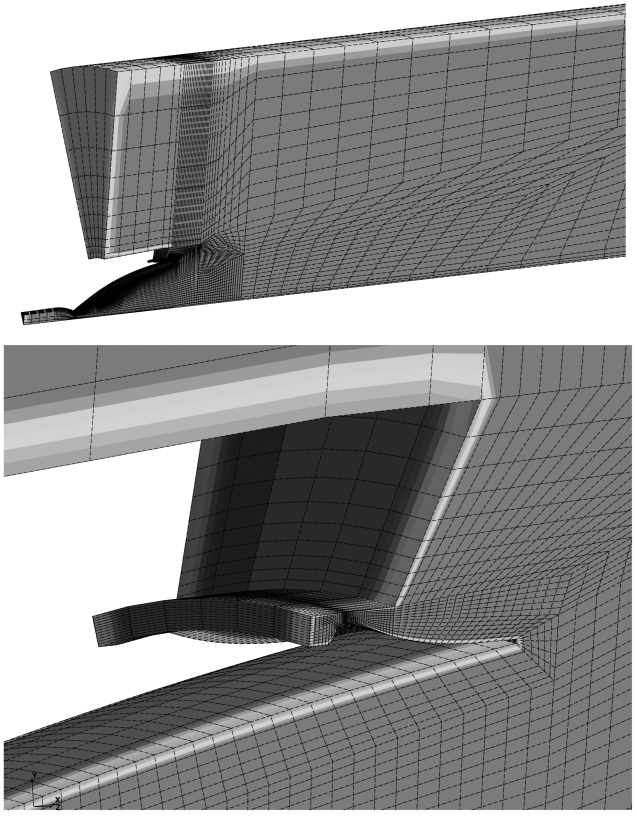

Fig. 4 Mesh of the three-dimensional model (upper) and detail of the aerospike nozzle, including actual geometrical features of the subscale nozzle (lower).

C. Three-Dimensional Model for Dump Configurations

To check if similar results could be achieved with a classical dump cooling exhaust flow, a similar three-dimensional CFD model was set up. In that model the annular aerospike is replaced by a classical holes' range, representative of typical dump cooling ejection technology. Main jet stagnation pressure and temperature are the same that those used for previous computations, while stagnation pressure of secondary flow has been increased, compensating the difference in equivalent throat area. The first computation was performed considering a dump cooling stagnation pressure equal to 24 bar, which allows maintaining the same mass flow rate used for the aerospike test case. At these operating conditions, the main jet is still in separated conditions, even if the presence of the dump flow is responsible of the forward displacement of the separation line. Subsequently, the stagnation pressure of the dump flow was progressively increased, up to 75 bar. In these conditions, the separation point moves toward the nozzle exit, until it becomes stable at around nine tenths of the nozzle length ($X/L = 0.9$). Further increase of the dump stagnation pressure does not improve the separation characteristics.

Figure 6 shows the most advance position of the separation line computed with classic dump flows. It is important to note that the main nozzle plume cannot reach full-flowing conditions at the given operating conditions.

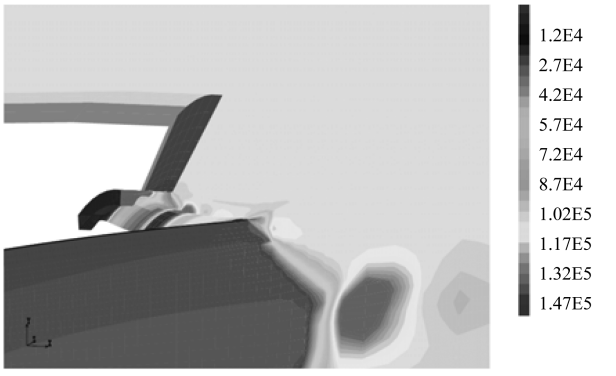

Fig. 5 Detail of the pressure field (Pa) at nozzle exit plane with operating aerospike.

IV. Experimental Verification

Taking into account encouraging two-dimensional and three-dimensional CFD results obtained for different TOC profiles, an affordable experimental verification of the new nozzle concept was decided. A low cost, blow-down, pressure regulated test setup has been designed, manufactured and assembled in a short delay. The main nozzle is a high precision machined assembly, made of aluminum and instrumented with static pressure taps and thermocouples. A heating system has been implemented on the feeding line, upstream of the nozzle convergent part, in order to prevent condensation of residual humidity at the highest expansion ratio. Security devices (relief valves) have also been implemented, in order to guarantee safe test conditions. Measurements have been acquired with National Instrument standard components. Pressure measurements have been acquired at 100 Hz, temperature measurements at 1 Hz. Eight bit resolution is used for both pressure and temperature measurements. The experimental campaign was primarily intended to verify the actual behavior of the new nozzle concept. Additionally, robustness of the expected flow field configuration with respect to feeding conditions disturbances and transient phases was also checked.

A. Test Configuration

The model used for the test activities is an aluminum nozzle, manufactured in three separated parts which are bolted together before performing the final machining of the inner contour, in order to guarantee a smooth and continuous profile (Figs. 7 and 8). The nozzle profile is the same used for three-dimensional computations. The aerospike inner profile is a skewed parabola directly machined on the external surface of the final segment of the main nozzle (see Fig. 8). The aerospike shroud is machined on the third part composing the model. The aerospike plenum chamber is obtained by

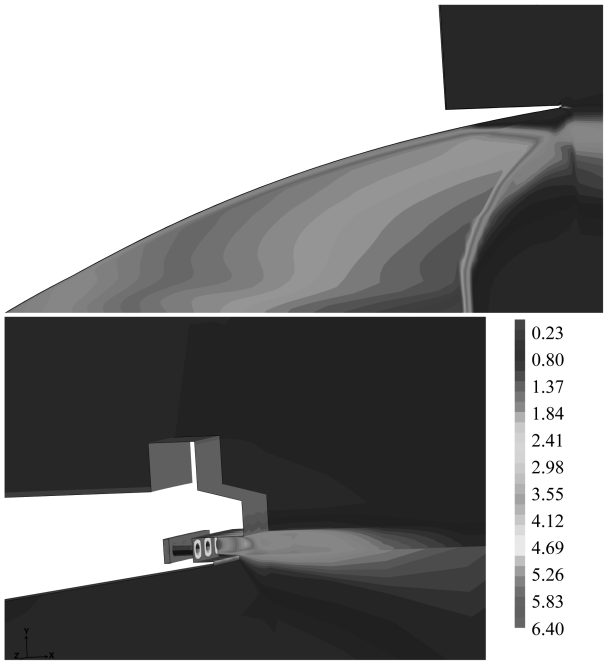

Fig. 6 Main nozzle Mach field (upper) and detail of the dump cooling discharge area (dump stagnation pressure, 75 bar) (lower).

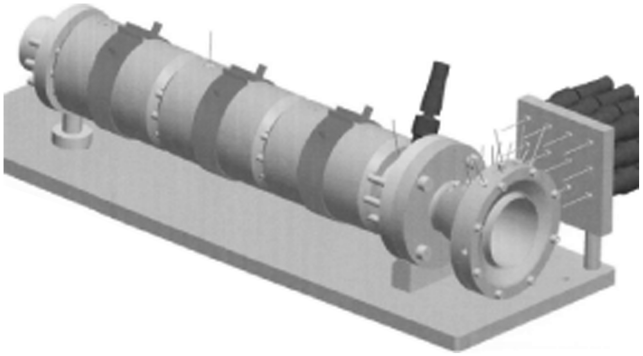

Fig. 7 Experimental setup: assembly.

assembling together the second and third parts. A special design of these two segments ensures uniform tangential distribution of the working fluid, which is primarily delivered by two opposite feeding lines. The main characteristics of the device are as follows: main nozzle throat radius = 8 mm; main nozzle outlet radius = 45.2 mm; main nozzle length = 120 mm; aerospike throat height = 0.3 mm; aerospike inner wall length (spike) = 13.84 mm; aerospike outer wall length (shroud) = 4.24 mm.

The rather small dimensions of the nozzle and the critical position of some pressure transducers (measurement points located at the end of the main nozzle profile as well as on the aerospike inner profile had to be machined in very thin metallic parts) impose a radial accommodation of the aerospike feeding chamber (see Figs. 8 and 9). Consequently, a large solid surface (not reflecting the actual geometry of a full-scale nozzle) is generated around the aerospike outer lip. To verify that this large flange does not introduce prejudicial flow perturbations, a pressure transducer is implemented near the lip of the aerospike shroud (Fig. 10). Accordingly, the actual geometry of the test hardware has been implemented in the three-dimensional CFD model, in order to take into account any potential effect due to the presence of this additional surface.

The model is equipped with 13 pressure taps and 2 thermocouples, distributed as shown in Fig. 11. A high pressure transducer (transducer A) and one thermocouple (transducer T1) measure the stagnation pressure and temperature of the main jet, respectively. One pressure transducer (1–16 bar) measures the secondary flow stagnation pressure (transducer F); seven pressure transducers (0–3 bar) are used to monitor the main jet wall pressure distribution (transducers B–E and M, L, K); two pressure transducers (0–3 bar) measure the wall pressure distribution over the aerospike inner wall (transducers I and J); one pressure transducer (0–3 bar) measures the wall pressure near the aerospike outer wall lip (transducer G); one pressure transducer (0–3 bar) measures the wall pressure on the front wall, near the aerospike outer wall lip (transducer H).

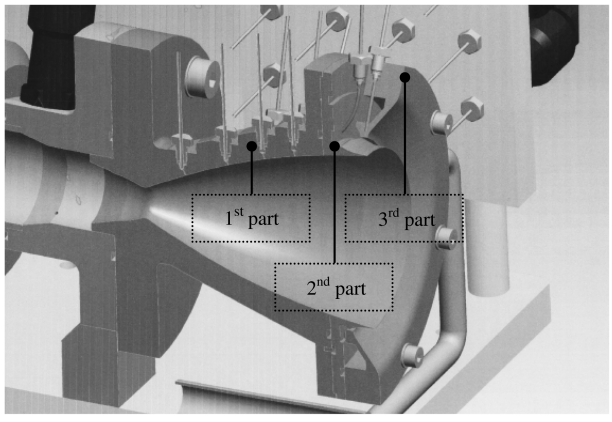

Fig. 8 Detail of the nozzle.

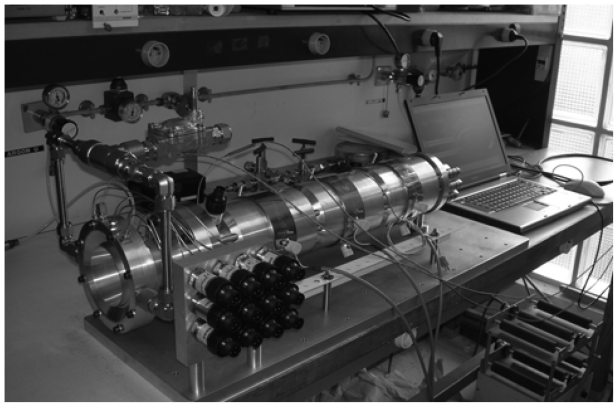

Fig. 9 Experimental arrangement during transducers calibration.

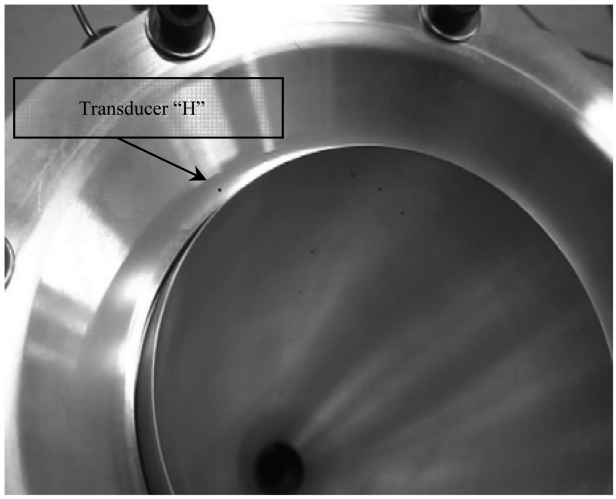

Fig. 10 Transducers H measuring point.

B. Test Campaign

Few preliminary tests have been initially performed in order to check the global behavior of the test setup. Then, a series of nine tests has been performed in order to investigate the effectiveness of the proposed concept. Table 1 summarizes the operating conditions requested for the test series.

Each test has been performed in blow-down conditions, using high pressure bottles filled with compressed air and setting the initial stagnation pressure level of the main nozzle by means of a manual pressure regulator. Allowable test duration was in the range 7–14 s, depending on the performed operational point. The secondary flow was independently fed: because of the low mass flow rate, very stable feeding conditions could be maintained.

Figure 12 shows a typical time evolution of the stagnation pressure signals for the main jet and the aerospike flow (three activations), during a test. It may be observed that, due to the blow-down effect, the stagnation pressure of the main jet varies between 7 and 18%

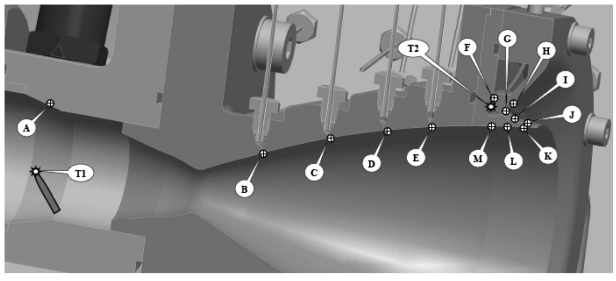

Fig. 11 Transducer implementation.

Table 1 Performed tests

Test number	Main jet stagnation pressure, bar	Secondary flow stagnation pressure, bar
1	——	5
2	——	8
3	——	12
4	40 – 30	——
5	75 – 30	——
6	60 – 40	5
7	46 – 21	5 – 0 – 5 – 0 – 5
8	48 – 29	5
9	60 – 33	6

during each operative phase of the aerospike. Such a decrease of the stagnation pressure does not change the structure of the supersonic flow in the main nozzle. Consequently, it is possible to conclude that the changes observed on the pressure profile (pressure transducers B–E and M, L, K (see Figs. 13–18), at each activation of the aerospike jet, are only due to the action of the fluidic barrier generated by the secondary flow. Figures 13 and 16 show typical pressure profiles (computation results and measurement points) that are obtained for test conditions without and with secondary flow, respectively.

V. Analysis of Experimental Results

Transducers M and K have been used to assess the nozzle behavior (note that K transducer is the nearest to the nozzle exit plane).

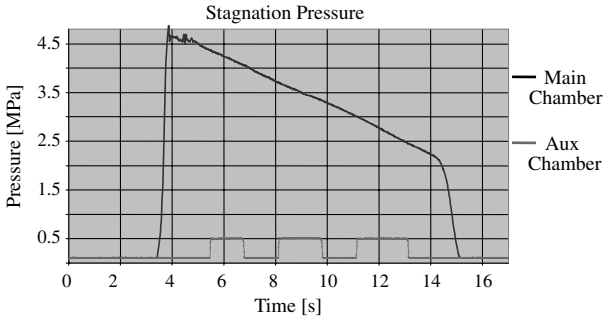

Fig. 12 Plot of stagnation pressure measurements: test 7.

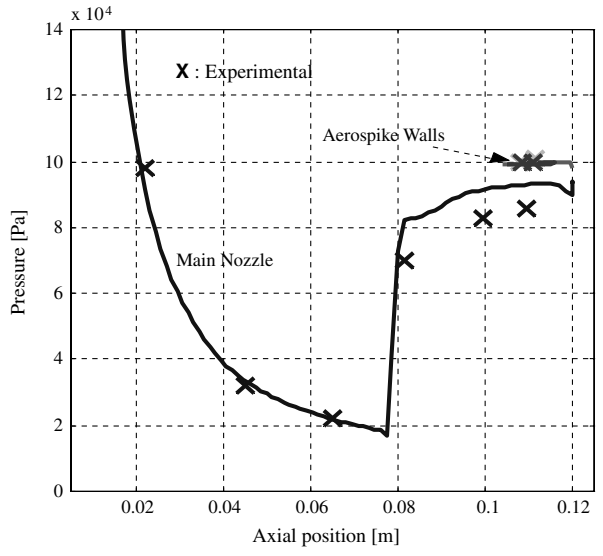

Fig. 13 Wall pressure profile: test 7, NPR = 37, *w/o* secondary jet.

Figure 13 shows the comparison between experimental data and computed wall pressure profile for the following operating conditions: main jet stagnation pressure $(P_i) = 37$ bar; the aerospike flow was not activated.

At these operating conditions, large flow separation occurs inside the main nozzle. Experimental and numerical results are in good agreement and, according to numerical results, separation occurs at $X/L = 0.64$.

Figures 14 and 15 show the computed pressure and Mach fields, respectively. Figure 16 shows the comparison between experimental data and computed wall pressure profile for the same main nozzle operating conditions, when annular aerospike is operating: main jet stagnation pressure $(P_i) = 37$ bar; aerospike stagnation pressure $(P_{ij}) = 6$ bar.

All the transducers give evidence of an attached flow and the measured pressure levels are in good agreement with computed wall pressure (down to 17,500 Pa). Computed pressure and Mach fields for these operating conditions are showed in Figs. 17 and 18, respectively. Other operating points (main nozzle NPR = 39, with and without aerospike flow; main nozzle NPR = 53.8, with and without aerospike flow) have also been analyzed. Good agreement between experimental and numerical results is confirmed for all the operating conditions.

It may be noticed that, when flow separation occurs in the main nozzle, the predicted compression wave is stronger than the measured values. Mesh refinement around the separation area can easily improve the prediction. Nevertheless, the position of the separation line is correctly computed and correct pressure values are obtained on the external surfaces (aerospike surface). On the contrary, when the aerospike jet is operated, computed wall pressure distribution matches almost perfectly the experimental values, both for main nozzle and aerospike surfaces. Moreover, large pressure variations are observed along the aerospike wall, due to the recompression waves reflecting on the spike surface. This is a clear evidence of the not optimized design of the aerospike profile. It

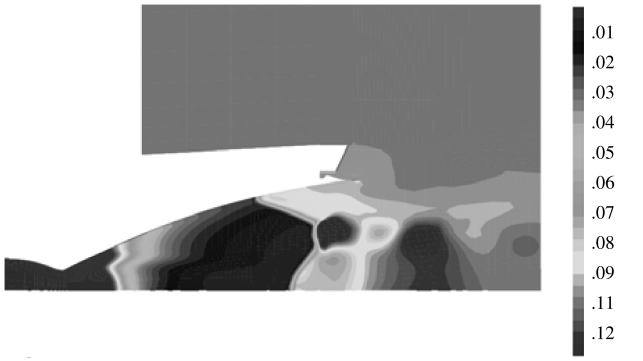

Fig. 14 Computed pressure field (MPa): test 7, NPR = 37, *w/o* secondary jet.

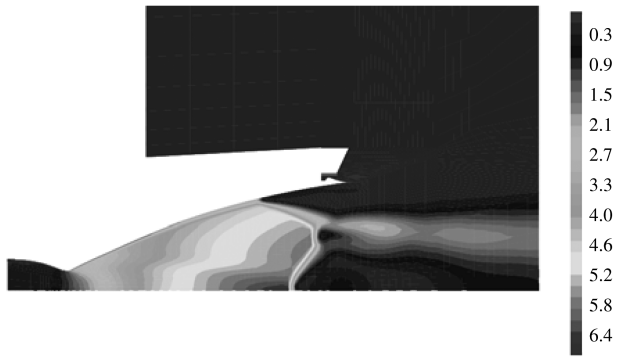

Fig. 15 Computed Mach field: test 7, NPR = 37, *w/o* secondary jet.

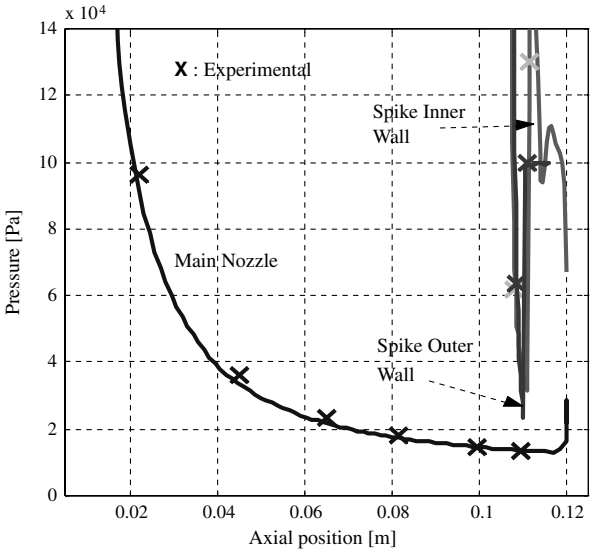

Fig. 16 Wall pressure profile: test 9, NPR = 37, aerospike stagnation pressure $P_{ij} = 6$ bar.

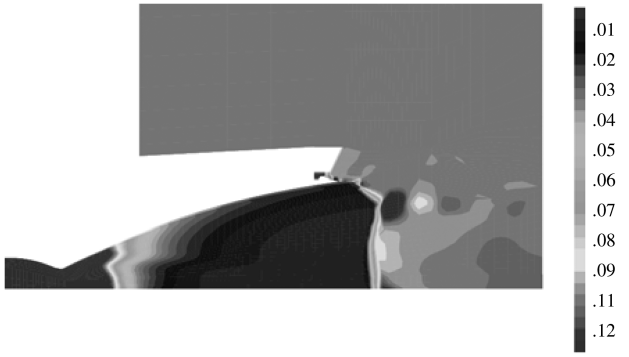

Fig. 17 Computed pressure field (MPa): test 9, NPR = 37, aerospike stagnation pressure $P_{ij} = 6$ bar.

supports the idea that the proposed concept has large potential for even better performances.

Because of the limitations imposed by the size of the experimental model, only a limited number of pressure taps could be implemented. However, the agreement between computed pressure profiles and measured values for the selected operating conditions is rather remarkable.

These tests experimentally prove the effectiveness of the new concept, demonstrating that full-flowing conditions can be maintained in the main nozzle at NPR = 37, i.e., about 50% of nominal full-flowing NPR value (75).

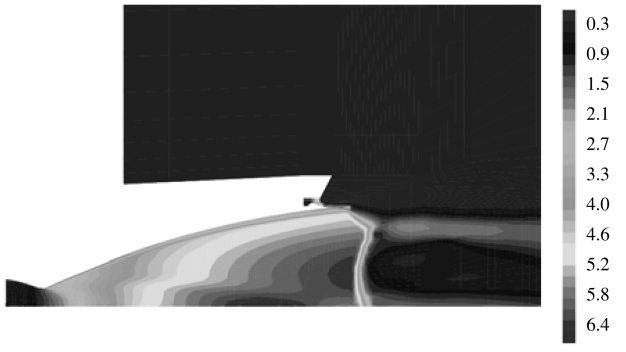

Fig. 18 Computed Mach field: test 9, NPR = 37, aerospike stagnation pressure $P_{ij} = 6$ bar.

The aerospike consumption needed to obtain this remarkable result is around 5% of the mass flow rate flowing through the main nozzle, at nominal full-flowing NPR.

Transducer H, used to monitor the pressure field near the aerospike shroud, always measured unchanged atmospheric ambient pressure (1 bar). Similarly, numerical simulations did not give evidence of significant perturbations introduced by the external geometry of the experimental device, demonstrating that the specific design of the experimental device does not influence the obtained results.

Figures A1–A4, in appendix, compare flow visualizations during tests (pictures taken from a hand camera) and computed Mach fields for two operating conditions, with and w/o activated annular aerospike. Spontaneous condensation of residual water vapor contained in the main jet (bright white area, delimited by dashed lines in Figs. A1 and A3) helps to visualize the size of the plume. The wider jet is obtained when the aerospike is activated: its size corresponds to the outlet diameter of the main nozzle.

Significant effect of the aerospike flow on the main nozzle behavior is observed also during transient phases. The major change is measured during the shut-down phase, when the presence of the aerospike flow delays the flow separation appearance and induces a restricted shock separation (RSS) configuration, which has never been observed before, for this specific profile in cold flow experiments.

It should be noted that side loads generated by the transition from FSS to RSS (and vice versa) can develop only in case the said transition happens in unsymmetrical manner. If the transition is symmetric, side loads do not develop. The presence of the aerospike jet only forces the transition, without generating any unsymmetrical condition. Moreover, FSS to RSS transition is a quite fast phenomenon [14]: associated side loads are characterized by high frequencies, which are usually not very harmful for the nozzle structure. On the contrary, the most dangerous side loads are those developing at low frequency, generated by the distortion of the separation line [25,29,31] and which are usually observed in FSS conditions or when a closed recirculating bubble, characteristic of the RSS configuration, unsymmetrically opens at the nozzle exit plane. In this respect, the presence of the aerospike jet does not represent an aggravating factor for transient side loads: it can force symmetric FSS–RSS transition, while avoiding uncontrolled distortion of the separation line.

VI. Nozzle Behavior in Reacting Conditions

On the basis of the encouraging results obtained in cold gas conditions and taking into account the good agreement between numerical and experimental results, three-dimensional CFD computations have been used to verify the performances of the proposed nozzle concept in hot firing conditions.

A seven species (H_2, O_2, OH, H, O, H_2O, N_2) reaction model TECK combustion scheme using EKLUND kinetics, see [24,25], has been used to describe the finite-rate chemical kinetics.

The same mesh, previously used for three-dimensional cold gas computations, has been used for the hot firing cases. This choice is justified on the basis of previous works, carried out with the same CFD tool (see [25]), and by the fact that the original mesh is already well refined, in particular in the area around the nozzle tip (typical cell size: $1 \times 1 \times 0.5$ mm), for the specific purpose of this study. In addition, a sensitivity study has been performed on a two-dimensional mesh, which confirmed that the chosen cell size is well adapted for this computation.

Boundary conditions have been set in terms of feeding conditions for the combustion chamber (propellants pressure and temperature level, mixture ratio) and for the secondary flow (pressure and temperature levels, pure Hydrogen flow). Ambient air, at sea level conditions, is taken into account as surrounding fluid (pressure and temperature levels, chemical composition). A perfectly premixed propellant mass flow is considered (injection head is not meshed): the injection pattern is deemed not to be a critical parameter for the nozzle efficiency.

Steady-state and transient (start-up and shut-down) computations have been carried out. For both types of computations gaseous propellant inlet conditions have been chosen. Indeed, despite the capability of the CPS-C code to handle variable thermodynamic properties over very large temperature and pressure ranges (including supercritical and transcritical thermodynamic conditions), the computational complexity related to phase change mechanism has been omitted, as these physical phenomena are not directly linked to the flow separation issue. Indeed, the combustion process taking place in the combustion chamber is mostly completed before the flow enters the sonic throat. Previous studies demonstrated that macroscopic combustion heterogeneities (due to injector path or to mixture ratio distribution across the injection plate) can have a minor effect on the local position of the flow separation line along the nozzle circumference. Nevertheless, this aspect is covered in this study by the transient computation: the combustion pressure ranges from few bar to the full-flowing conditions and the obtained results can be intended as the local worst case for the effectiveness of the proposed concept.

A. Steady-State Computations

Three-dimensional steady-state computations have been carried out in order to characterize the nozzle behavior when operating with and w/o the secondary flow. Several test cases have been computed, progressively increasing the combustion chamber pressure, in order to achieve the following three relevant operating conditions:

Case 1: minimum combustion chamber pressure level providing full-flowing nozzle, w/o secondary flow.

Case 2: minimum combustion chamber pressure level providing full-flowing nozzle, with secondary flow.

Case 3: same pressure level as in case 2, without secondary flow occurrence of flow separation.

In the absence of the secondary flow, the full-flowing conditions are achieved for combustion chamber pressure level equal to 10.9 MPa (109 bar). When the secondary flow is activated (hydrogen stagnation pressure equal to 0.75 MPa; hydrogen stagnation temperature equal to 700 K), the minimum combustion chamber pressure level allowing full-flowing conditions is 6.8 MPa (68 bar) (Fig. 19).

Based on these results, the efficiency of the flow separation control device is also confirmed in hot reacting conditions.

Potential post combustion phenomena occurring at the nozzle exit area have been checked. When the secondary jet is not operated, there is a small zone, starting at the tip of the nozzle wall and developing downstream, where a moderate reaction rate can be observed. This is due to the confluence of the main jet, rich in hot fuel, with the oxygen of ambient air. When the secondary flow is activated, the reaction rate is less intense and the reaction zone moves further downstream. This is due to the presence of the outer hydrogen flow, ejected by the aerospike, which prevents the hot plume to be directly in contact with oxygen contained in ambient air.

B. Transient Computations

A transient three-dimensional computation has also been carried out in order to verify the start-up and shut-down behaviors of the new nozzle concept. Following boundary conditions have been implemented: for the main combustion chamber, hydrogen inlet temperature is set at 200 K; oxygen inlet temperature is set at 300 K. The feeding pressure varies from 0.1 to 11.8 MPa (upward and downward; steady-state operation plateau at 118 bar) for both propellants, with a pressure rise time of 0.1 s (representative of typical rise times for rocket engines, taking into account reduced geometrical scales (see [29,31]). Oxidiser/fuel mixture ratio is kept constant, equal to seven. The annular aerospike is fed with pure hydrogen, with total temperature of 700 K (constant). The hydrogen feeding pressure is set at 0.75 MPa (constant).

The time step used for transient computations has been set to 1E (7 s).

According to the obtained results, the full-flowing conditions are achieved at around $T = 0.06$ s, which corresponds to a combustion chamber pressure of about 7.4 MPa (74 bar). Taking into account that from steady-state computations full-flowing conditions in absence of the annular jet are achieved at a combustion chamber pressure of about 10.9 MPa (109 bar), the efficiency (with respect to flow separation phenomena) of the proposed nozzle concept is confirmed to be very high also in hot firing conditions. In addition, no significant

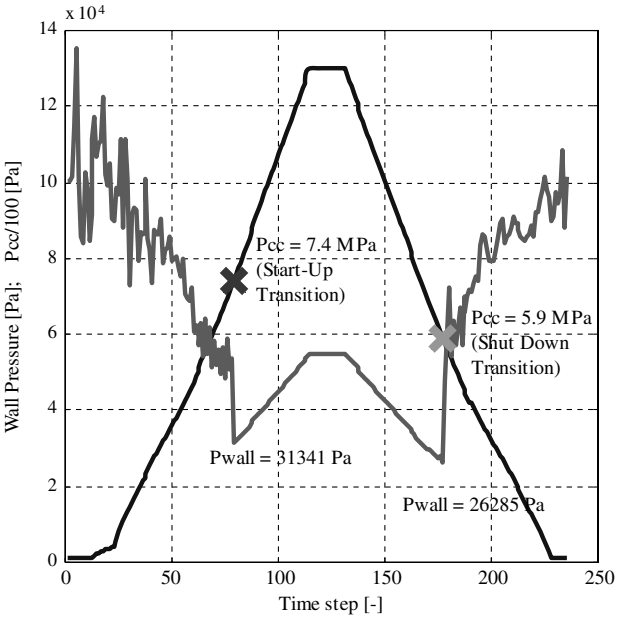

Fig. 20 Computed evolution of main chamber (P_{cc}) and nozzle wall (P_{wall}: computed at nozzle tip) pressure levels during start-up and shut-down transients. P_{wall} is computed at nozzle tip.

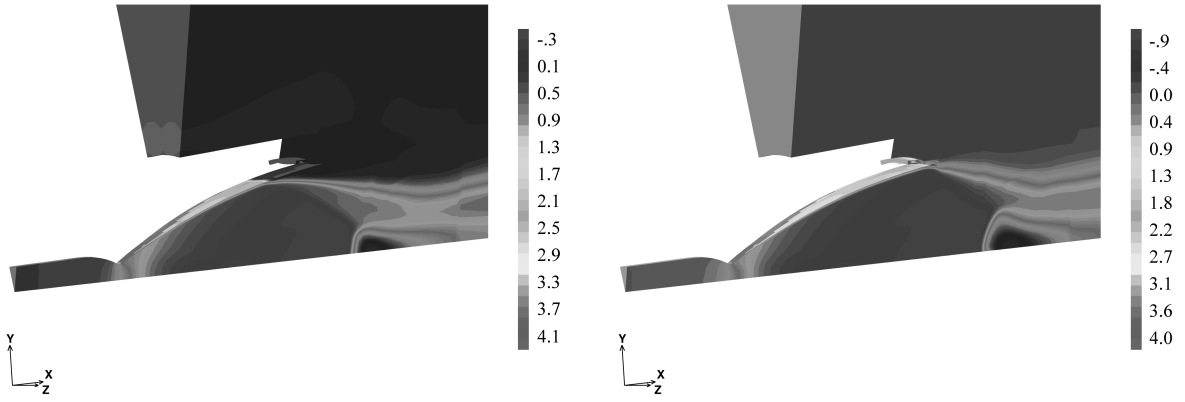

Fig. 19 Longitudinal velocity (10^3 m/s) at $P_{cc} = 6.8$ MPa: without secondary flow (left) and with secondary flow (right).

dynamic effect is observed with regard to steady-state computations. When considering the shut-down transient, the efficiency of the nozzle is observed to be even higher: full-flowing conditions are maintained for a combustion chamber pressure level down to 5.4 MPa (54 bar). Such a hysteresis, already observed in flow separation phenomena [32], provides even more robustness to the new nozzle concept. Indeed, once the full-flowing conditions are achieved, even large NPR oscillations cannot affect the established nozzle operating mode (see Fig. 20 and A5 in the appendix).

VII. Conclusions

A new nozzle concept is proposed in this paper. It is based on a classical bell-shaped nozzle, which is a well-known and worldwide-flight-proven concept, slightly modified by the addition of a small aerospike, which is implemented near the exit plane of the main nozzle. The behavior of this new concept has been verified by CFD computations and subscale cold gas experiments.

The new design allows a better optimization of the nozzle expansion ratio, even for main stage or booster engines, in order to achieve higher vacuum-specific impulse values, without incurring in flow separation problems at sea level. Indeed, the proposed design allows reaching wall pressure values of around 17,000 Pa in full-flowing conditions at sea level, i.e., much less than typical pressure levels observed in classic nozzle. Accordingly, the expansion ratio of booster engine nozzles can be increased (maintaining the same combustion chamber pressure), allowing an Isp gain with respect to present performances.

Computational results and experimental measurements suggest that this new concept can allow a wide throttling range at low altitude, without incurring in flow separation phenomena and associated side loads. Potentiality for favorable behavior even during transient phases, allowing significant reduction on transient side-loads activity, is suggested by the available data. This topic will be investigated more in detail in future works.

Computed test cases in reacting conditions (hot gases) confirm the great potential of the proposed nozzle concept for full-scale applications. Unfortunately, experimental data in hot firing conditions are not yet available. Nevertheless, the same CFD code has already been used in the past for several applications in rocket engine science (combustion, cooling, flow separation, propellant management) and good agreement was found between experimental data and computational results, allowing good confidence on results presented in this work.

Appendix: Additional Results

Fig. A1 Test 9, NPR = 37, aerospike stagnation pressure $P_{ij} = 6$ bar.

Fig. A2 Test 9, computed Mach field, NPR = 37, aerospike stagnation pressure $P_{ij} = 6$ bar.

Fig. A3 Test 9, NPR = 35, w/o secondary jet.

Fig. A4 Test 7, computed Mach field, NPR = 37, w/o secondary jet.

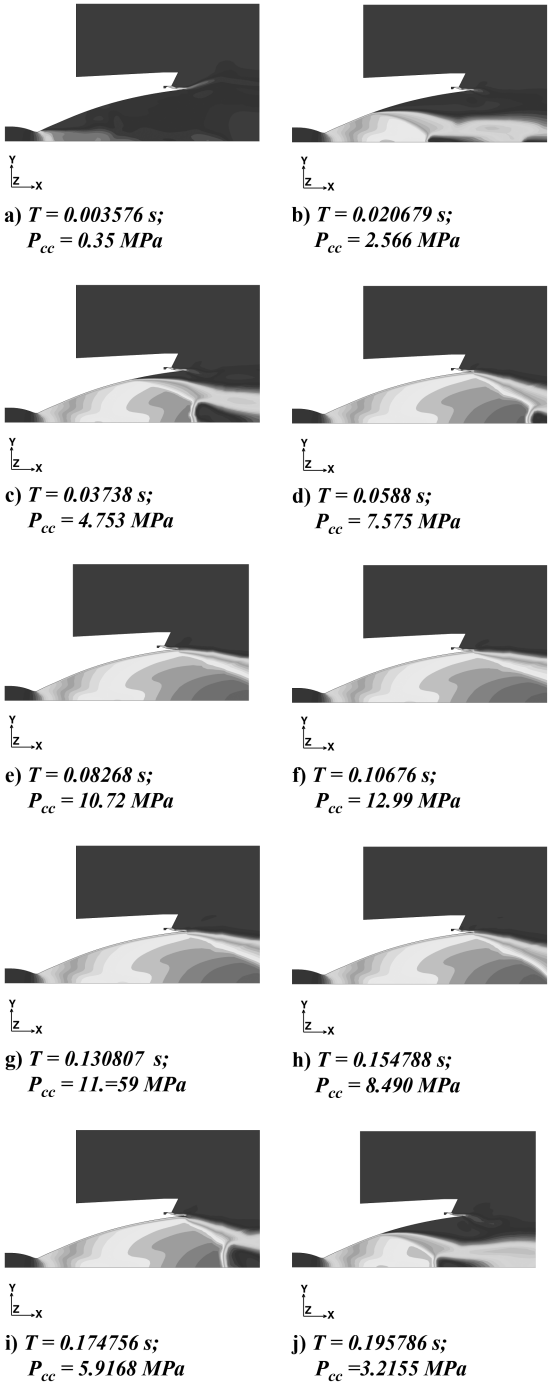

Fig. A5 Computed Mach field: start-up and shut-down transients in reacting conditions.

Acknowledgments

The experimental work has been funded by Centre National dEtudes Spatiales (CNES). The author would like to thank M. Pons (CNES) for his suggestion; F. Cahuzac and M. Illig (CNES) for their support, in particular during the preparation and the execution of the experimental campaign; J. Duval (ATMOSTAT) and all his team for their invaluable work; and the people at HP systems for their help. A special thanks to L. Lequette (BERTIN Technologies), for his suggestions and constructive remarks.

The new rocket nozzle concept has been patented under the number 07-58812 FR, international application number PCT/FR2008/052004. The new rocket engine nozzle is known under the acronym of *BOCCAJET* (bell optimized nozzle controlled by coaxial aerospike jet).

References

[1] Chapman, D., Huehn, D., and Larson, H., "Investigation of Separated Flows in Supersonic and Subsonic Streams with Emphasis on the Effect of Transition," NACA Rept. 1536, Ames Aeronautical Lab., Moffet Field, CA, 1958.

[2] Frey, M., Preuss, A., Hagemann, G., Girard, S., Alziary, T., Reijasse, P., Stark, R., Hannemann, K., Schwane, R., Perigo, D., Boccaletto, L., and Lambare, H., "Joint European Effort Toward Advanced Rocket Thrust Chamber Technology," Sixth International Symposium on Launcher Technologies, Munich, Germany, 8–11 Nov. 2005.

[3] Reijasse, P., Kachler, T., Boccaletto, L., and Lambare, H., "Afterbody and Nozzle Aerodynamics for Launchers Through the CNES-ONERA ATAC Programme," Sixth International Symposium on Launcher Technologies, Munich, Germany, 8–11 Nov. 2005.

[4] Shi, J., "Rocket Engine Nozzle Side Loads Transient Analysis Methodology: A Practical Approach," 46th AIAA/ASME/ASCE/AHS/ASC Structures, Structural Dynamics and Materials Conference, AIAA Paper 2005-1860, Austin, TX, 18–21 April 2005.

[5] Papamoschou, D., and Johnson, A., "Unsteady Phenomena in Supersonic Nozzle Flow Separation," 36th AIAA Fluid Dynamics Conference and Exhibit, AIAA Paper 2006-3360, San Francisco, CA, June 2006.

[6] Smalley, K., Brown, A., Ruf., J., and Gilbert, J., "Flow Separation Side Loads Excitation of Rocket Nozzle FEM," 48th AIAA/ASME/ASCE/AHS/ASC Structures, Structural Dynamics and Materials Conference, AIAA Paper 2007-2242, Honolulu, HI, 23–26 April 2007.

[7] Ruf, J., McDaniels, D. M., and Brown, A. M., "Nozzle Side Load Testing and Analyses at MSFC," 45th AIAA/ASME/SAE/SEE Joint Propulsion Conference, AIAA Paper 2009-4856, Denver, CO, 2–5 Aug. 2009.

[8] Sato, M., "Characteristics of Dynamics Load on Nozzle Extension," 56th International Astronautical Congress of the International Astronautical Federation, the International Academy of Astronautics and the International Institute of Space Law, IAC Paper 05-C4.2.06, Fukukoa, Japan, 17–21 Oct. 2005.

[9] Watanabe, Y., Sakazume, N., Yonezawa, K., and Tsujimoto, Y., "LE-7A Engine Nozzle Flow Separation Phenomenon and the Possibility of RSS Suppression by the Step Inside the Nozzle," 40th AIAA/ASME/SAE/ASEE Joint Propulsion Conference and Exhibit, AIAA Paper 2004-4014, Fort Lauderdale, FL, 11–14 July 2004.

[10] Stark, R., "Flow Separation in Rocket Nozzles, a Simple Criteria," 41st AIAA/ASME/SAE/SEE Joint Propulsion Conference, AIAA Paper 2005-3940, Tucson, AZ, 10–13 July 2005.

[11] Spaid, F. W., and Frishett, J. C., "Incipient Separation of a Supersonic, Turbulent Boundary Layer, Including Effect of Heat Transfer," *AIAA Journal*, Vol. 10, No. 7, 1972, pp. 915–922. doi:10.2514/3.50245

[12] Summerfield, M., Forster, C., and Swan, W., "Flow Separation in Over-Expanded Supersonic Exhaust Nozzles," *Jet Propulsion*, Vol. 24, Sept. 1954, pp. 319–320.

[13] Délery, J. M., "Topologie des Écoulements Tridimensionnels Décollés Stationnaires: Points Singuliers, Séparation et Structures Tourbillonnaires," ONERA RT 121/7078 DAFE/N, 1999.

[14] Östlund, J., and Bigert, M., "A Subscale Investigation on Side Loads in Sea Level Rocket Nozzle," 35th AIAA/ASME/SAE/ASEE Joint Propulsion Conference and Exhibit, AIAA Paper 1999-2759, Fort Lauderdale, FL, 20–24 July 1999.

[15] Semenov, V. V., Finogenov, S. L., Ivanov, I. E., Krykov, I. A., and Talalayev, A. A., "Liquid Propulsion with Altitude Compensation Concept Trade Study," 57th International Astronautical Congress of the International Astronautical Federation, the International Academy of Astronautics and the International Institute of Space Law, IAC Paper 06-C4.1.09, Valencia, Spain, 2–6 Oct. 2006.

[16] Nürnberger-Génin, C., and Stark, R., "Experimental Study of Dual Bell Nozzle," Second European Conference for Aerospace Science (EUCASS), Bruxelles, Belgium, July 2007.

[17] Sato, M., Moriya, S., Tadano, M., Sato, M., Masuoka, T., and Yoshida, M., "Experimental Study on Transitional Phenomena of Extendible Nozzle," 43rd AIAA/ASME/SAE/ASEE Joint Propulsion Conference and Exhibit, AIAA Paper 2007-5471, Cincinnati, OH, 8–11 July 2007.

[18] Besnard, E., and Garvey, J., "Development and Flight-Testing of Liquid Propellant Aerospike Engines," 40th AIAA/ASME/SAE/ASEE Joint Propulsion Conference and Exhibit, AIAA Paper 2004-3354, Fort Lauderdale, FL, 11–14 July 2004.

[19] Goetz, A., Hagemann, G., Kretschmer, J., and Schwane, R., "Advanced Upper Stage Propulsion Concept: The Expansion Deflection Upper Stage," 41th AIAA/ASME/SAE/ASEE Joint Propulsion Conference and Exhibit, AIAA Paper 2005-3752, Tucson, AZ, 10–13 July 2005.

[20] Verna, S. B., Stark, R., Nuerenberger-Genin, C., and Haidn, O., "Flow Separation Studies During the Transition Modes of a Sub-Scale Dual-Bell Nozzle," 45th AIAA/ASME/SAE/SEE Joint Propulsion Conference, AIAA Paper 2009-4854, Denver, CO, 2–5 Aug. 2009.

[21] Niu, K., Yonezawa, K., Ishizaka, K., and Kimura, T., "Experimental and Analytical Study for Design of Dual-Bell Nozzles," 45th AIAA/ASME/SAE/SEE Joint Propulsion Conference, AIAA Paper 2009-5149, Denver, CO, 2–5 Aug. 2009.

[22] Niu, K., Yonezawa, K., Ishizaka, K., and Kimura, T., "Control of Transition between Two Working Modes of a Dual-Bell Nozzle by Gas Injection," 45th AIAA/ASME/SAE/SEE Joint Propulsion Conference, AIAA Paper 2009-4952, Denver, CO, 2–5 Aug. 2009.

[23] Östlund, J., and Muhammad-Klingmann, B., "Supersonic Flow Separation with Application to Rocket Engine Nozzle," *Applied Mechanics Reviews*, Vol 58, May 2005, pp. 143–177. doi:10.1115/1.1894402

[24] CPS-C Software Package, Ver. 5.9, Bertin Technologies, 2009.

[25] Boccaletto, L., and Lequette, L., "CFD Computation for Rocket Engines Start Up Simulation," 41st AIAA/ASME/SAE/SEE Joint Propulsion Conference, AIAA Paper 2005-4438, Tucson, AZ, 10–13 July 2005.

[26] Durbin, P. A., "Separated Flow Computations with the k-epsilon-v-Squared Model," *AIAA Journal*, Vol. 33, No. 4, 1995, pp. 659–664. doi:10.2514/3.12628

[27] Poroseva, S., and Iaccarino, G., "Simulating Separated Flows Using the k-ε Model," *Annual Research: Briefs 2001*, http://ctr.stanford.edu/ResBriefs01/poroseva2.pdf.

[28] Kalitzin, G., Medic, G., Iaccarino, G., and Durbin, P., "Near-Wall Behaviour of RANS Turbulence Models and Implications for Wall Functions," *Journal of Computational Physics*, Vol. 204, No. 1, 2005, pp. 265–291. doi:10.1016/j.jcp.2004.10.018

[29] Boccaletto, L., Reijasse, P., and Dussauge, J. P., "Dynamic Behaviour of a Separation Oblique Shock During Film Cooling Transient Injection," 37th AIAA Fluid Dynamic Conference and Exhibit, AIAA Paper 2007-4003, Hyatt Regency Miami, Miami, FL, 25–28 June 2007.

[30] Dunn, S. S., and Coats, D. E., "Optimum Nozzles Contours for Aerospike Nozzles Using the TDK 99 Computer Code," 36th JANNAF Combustion Subcommittee, Cocoa Beach, FL, 1999.

[31] Reijasse, P., and Boccaletto, L., "Nozzle Flow Separation with Film Cooling," 38th AIAA Fluid Dynamic Conference and Exhibit, AIAA Paper 2008-4150, Seattle, WA, 23–26 June 2008.

[32] Ponomarev, N. B., Komarov, V. V., and Ponomarev, A. A., "Experimental Investigations of Flow Restricted Shock Separation in High-Area-Ratio Nozzle with Exit Cone," 45th AIAA/ASME/SAE/SEE Joint Propulsion Conference, AIAA Paper 2009-5145, Denver, CO, 2–5 Aug. 2009.

K. Frendi
Associate Editor